FIG. 4. Chain of defects in InGaAsP LPE layer revealed by anodic oxidation.

oxide spot on the site while the background is almost free of oxide. Figure 4 shows the extreme of this phenomenon. A network of defects on the epitaxial layer is revealed. Avalanche photodiodes fabricated on these defects will have microplasma.

The use of the process described above can be extended to "patch" up all the leaky spots on a diode. If Schottky barrier or shallow junction diodes are to be fabricated on the quaternary epitaxial layer, the preferentially grown oxide spots will passivate the leaky spots of the diodes. Those leaky spots which if unpassivated are responsible for the localized breakdown of the diode are now localized metal-oxide semiconductor structures.

In conclusion, anodic oxides were successfully grown on InGaAsP quaternary materials in a 0.1-M ammonium phosphate dibasic solution. The grown oxides have refractive indices in the range of 1.6–1.75 which are suitable for antireflection coatings. The thickness of the oxide versus the cell voltage is linear and is approximately 22 Å/V. The breakdown field of the as-grown oxide is approximately 3×10^6 V/cm. The anodization on an epitaxial layer can be used as a nondestructive test to evaluate the quality of the layer and the "patching" up of the leaky spots of the layer.

The authors wish to thank Dr. P. D. Dapkus, Professor G. E. Stillman, and Dr. L. R. Tomaseta for their suggestions. The work is supported in part by Wright-Patterson AFB under Contract No. F33615-79-C-17171.

[1] J. J. Hsieh, J. Quantum Electron. **QE-15**, 694 (1979).
[2] H. Nishi, M. Yano, Y. Nishitani, Y. Ankita, and M. Takusagawa, Appl. Phys. Lett. **35**, 232 (1979).
[3] I. P. Kaminow, R. E. Nahory, M. A. Pollack, L. W. Stulz, and J. D. DeWinter, Electron. Lett. **15**, 763 (1979).
[4] C. E. Hurwitz and J. J. Hsieh, Appl. Phys. Lett. **32**, 487 (1978).
[5] H. D. Law, L. R. Tomasetta, and K. Nakano, Appl. Phys. Lett. **33**, 920 (1978).
[6] M. Feng, J. D. Obserstar, T. H. Windhorn, L. W. Cook, G. E. Stillman, and B. G. Streetman, Appl. Phys. Lett. **34**, 591 (1979).
[7] K. Nishida, K. Taguchi, and Y. Matsumoto, Appl. Phys. Lett. **35**, 251 (1979).
[8] B. Schwartz and W. J. Sundburg, J. Electrochem. Soc. **120**, 576 (1973).
[9] R. A. Logan, B. Schwartz, and W. J. Sundburg, J. Electrochem. Soc. **120**, 1385 (1973).
[10] H. Hasegawa, K. E. Forward, and Hans L. Hartnagel, Appl. Phys. Lett. **26**, 567 (1975).
[11] S. M. Spitzer, B. Schwartz, and G. E. Weigle, J. Electrochem. Soc. **122**, 397 (1975).
[12] H. D. Law and C. A. Lee, J. Electrochem. Soc. **123**, 765 (1976).
[13] S. Sakai, M. Umeno, T. Akoi, M. Tobe, and Y. Amemiya, Jpn. J. Appl. Phys. **18**, 1003 (1979).

Transition to faceting in multilayer liquid phase epitaxy of GaAs

Hans J. Scheel
IBM Zurich Research Laboratory, 8803 Rüschlikon, Switzerland

(Received 29 January 1980; accepted for publication 22 April 1980)

During deposition of *p*- and *n*-GaAs multilayers by a novel liquid phase epitaxy (LPE) technique on slightly misoriented substrates, a gradual transition from macroscopically stepped surfaces to faceting has been observed. The change from various different growth mechanisms on corrugated LPE-grown surfaces to a single one with propagating steps of heights of the order of 10 Å leads to extremely flat surfaces and to improved homogeneous dopant incorporation. These factors are likely to increase the performance of optoelectronic and microwave devices.

PACS numbers: 68.55. + b, 61.50.Jr, 81.15.Lm, 78.50.Ge

Very flat and structurally perfect surfaces are required (i) for active layers of less than 1000 Å of double-heterostructure (DH) lasers in order to increase efficiency and to reduce deterioration by dark regions due to surface ripples,[1] (ii) for quantum-well layer structures of the order of 150 Å, and (iii) for fabrication of GaAs field-effect transistors (FET's). Attempts to improve surface flatness in liquid phase epitaxy (LPE) have been (a) a small misorientation of

 0003-6951/80/130070-04$00.50

less than 0.1°;[2–6] (b) an optimal critical misorientation of 0.8° (Ref. 7) or 2° (Ref. 8) off {100} for GaAs and of 2.6° off {100} and 3.3° off {111} for InP,[9] (c) thin solution films, and (d) steep temperature gradients vertical to the substrate. The development of {100} or {111} facets has occasionally been observed in LPE of III-V compounds,[1–6,10,11] in most cases near the rim of substrates, whereas the central larger fraction of the surface was covered by macrosteps (terraces, treads and risers) or by waves (ripples or corrugations). Only rarely has the whole substrate been transformed into a facet.[2–5] In the present letter the gradual transition from a macroscopically stepped surface to the *flat* crystallographic facet is described. The change of growth mechanism and its influence on dopant incorporation are demonstrated. This *faceting transition* was observed reproducibly and will be illustrated here by two examples. Another example was shown in Fig. 6 of an earlier paper[12] but not recognized then: The facet starts from the center of the second layer, its traces to the periphery are seen faintly, and the third to the ninth layers grow exactly on facet.

The multilayer structures were fabricated by the novel sliding-free *MultiLPE* technique.[12] Two or more solutions are contained in the chambers of a concentric double-screw graphite device. They are transferred from one substrate to the next by simple rotation. In experiment No. L17A, two saturation and two growth substrates of GaAs ($\bar{1}\bar{1}\bar{1}$), chemically polished and of 4.9 mm diameter with 4 mm ϕ free surface, were used subsequent to being etched for 30 s in HF-HNO_3-H_2O 1:3:4. The ingredients of the two solutions (5 g Ga 5*N*, 0.335 g GaAs powder each, and 0.025 g Ge and 0.025 g Sn, respectively, for *p* and *n* doping) were introduced into

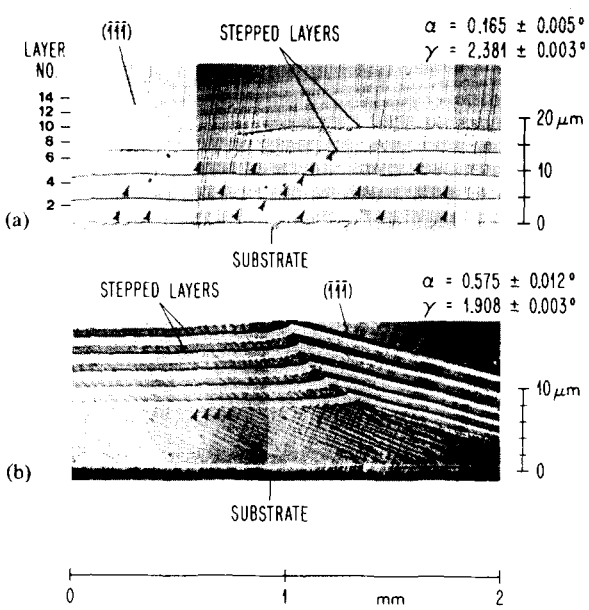

FIG. 1. Two examples of facetting transition for misorientation $\alpha = 0.165 \pm 0.005°$, cooling rate 3.5 °C h^{-1} and 10 min growth time per layer [Fig. 1(a)], and for misorientation $\alpha = 0.575 \pm 0.012°$, cooling rate 2 °C h^{-1} and 5 min growth time per layer [Fig. 1(b)]. Composite interference contrast (Nomarski) micrographs of the angle-lapped ($\gamma = 2.381°$ and 1.908°, respectively), and etched multilayer structures. The macrosteps (risers) are indicated by arrows.

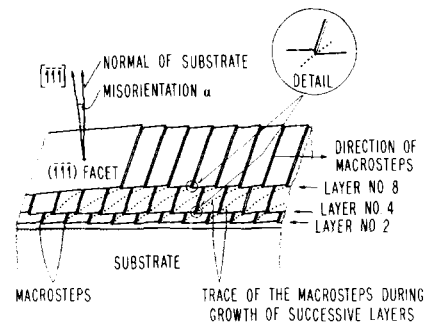

FIG. 2. Schematic presentation of the facetting transition [during growth of layers 7–12 of Fig. 1(a)]. The misorientation, the direction of the advancing macrosteps and their traces during growth of successive layers, are indicated. The vertical scale is extended due to the lapping angle γ (as in Fig. 1).

two separate chambers. The filled graphite device was inserted into a silica glass tube in a horizontal diffusion furnace with a 60-cm zone of constant temperature ($\pm < 0.1$ °C), and continuously flushed with Pd-diffused hydrogen. After one hour dissolution at 850 °C, under device oscillation, the saturation temperature 820 °C was set, and both solutions brought in contact with the saturation substrates for $1\frac{1}{2}$ h. Then the solutions were undercooled, in a neutral position, by 1.7 °C, moved to cover the growth substrates for ten minutes, and an additional cooling rate of 3.5 °C h^{-1} applied. By rotation of the whole graphite device, the solutions were transferred and exchanged and the second layers grown for ten minutes, and so on, until 15 layers had been deposited. After removal of the rest gallium from the substrate surface, the facets of 1.6–1.8 mm diameter were recognized (during aftergrowth the facet diameter decreased from about 3.2 mm). The multilayer structure was made visible by angle lapping at about 2° followed by *p-n*-selective etching with HNO_3-H_2O 1:9.[13] The lapping angle (and thus the vertical additional magnification) and the misorientation angle were determined by laser reflection and the coincidence of the facet with the crystallographic (111) plane proven by means of a combined laser and x-ray reflection technique, to be reported elsewhere.[14]

Figure 1(a), a Nomarksi interference contrast micrograph, shows the first six relatively flat layers (taking into account the difference between horizontal and vertical scales) grown parallel to the substrate surface, and the macrosteps (indicated by arrows) as well as their traces. [The difference in etching behavior at the macrosteps (risers) has been described by Saul and Roccasecca.[10] It is also seen in high-resolution photoluminescence measurements[1,15] and indicates a difference in impurity incorporation at macrosteps and terraces.] These are seen on the etched *p* layers only (Nos. 2,4,6), whereas in the unetched *n* layers the traces are not visible.

The macrosteps move parallel to the intersection of the substrate and the crystallographic ($\bar{1}\bar{1}\bar{1}$) plane (the facet).[2,4–6,10] The essential features of Fig. 1(a) are schematically illustrated in Fig. 2. After growth of seven layers, the transition to the facet is pronounced with the eighth layer, of which the left part [on Fig. 1(a) and 2] is facet and the right part still a terraced layer parallel to the misoriented sub-

strate surface. This facet grows from layer to layer until at layer No. 13 it covers the whole substrate (with the exception of a disturbed rim of 0.6 mm). The layer surfaces become extremely flat and parallel. The absence of growth features on the photograph (Fig. 1) indiates that any features would have heights of less than 1000 Å, which points to a change in growth mechanism. On several facets one observes (after about 12 μm aftergrowth) faint growth hillocks with a height of about 600 Å and a slope of about two seconds of arc (Talystep measurements) and growth steps of $\sim$20 Å height (Nomarski interference contrast microscopy). On one facet no growth hillock was visible, and a train of steps of height 10 Å or less and average distance 6 μm was found and is shown in Fig. 3. These steps originated from the facet/nonfacet interface. However, growth hillocks were also observed on terraces of stepped surfaces, and growth spirals made visible by decoration methods[16] or by multiple-beam interferometry.[17] Thus facets grow by microsteps originating from edges or growth hillocks, whereas on misoriented surfaces various surface nucleation mechanisms coexist, at least at low supersaturation. The expected growth-rate difference between facetted and stepped surfaces is well recognized from layer No. 8 of Fig. 1(a), where the two respective areas were grown under identical conditions and show a growth-rate ratio of 1:1.7. This may be the main cause for the change in the effective dopant distribution coefficient which, according to the visible etch intensity, is smaller for the facet compared to the nonfacet.

The effect of a relatively large misorientation angle (0.575°) on the faceting transition is shown with experiment L19B. With experimental conditions otherwise identical to L17A, a first thick layer was grown for 85 min (primary undercooling 0.5 °C, cooling rate 1 °C h^{-1}) and then 15 layers at a cooling rate of 2 °C h^{-1} and 5 min growth time per layer deposited. The microphotograph of the angle-lapped and etched multilayer structure is shown in Fig. 1(b). The explanation is similar to that of Fig. 1(a) except that a higher density of macrosteps is observed leading to a striationlike etch structure, especially in the first layer of about 7 μm thickness, and that the facet covers only half of the substrate owing to the large misorientation. The raised edge of the nonfacet at the intersection with the facet is explained by the locally increased supersaturation caused by the higher impedance of the growth on the adjacent facet.

In Table I the experimental data of experiments L17A and L19B, the misorientation angles, the thicknesses of the stepped and flat layers as well as the heights, the distances and the velocities of the macrosteps, are given. The latter data are in good agreement with theoretical values from a model of facet development and propagation.[18]

TABLE I. Measured values of layer thicknesses, growth rates of terraced and flat surfaces and their ratios, and of the heights and distances of the macrosteps for two experiments (L17A, L19B) with different cooling rates and substrate misorientations.

Experiment number	L17A	L19B
Misorientation α	0.165°	0.575°
Cooling rate	3.5 °C h^{-1}	2 °C h^{-1}
Initial undercooling	1.7 °C	0.5 °C
Growth time per layer	10 min	5 min
Terraced layers		
thickness	2.3 μm	1.3 μm[a]
growth rate v_s	38 Å s^{-1}	44 Å s^{-1}[a]
height of macrosteps	$\sim$0.26 μm	$\sim$0.16 μm[a]
distance of macrosteps	$\sim$350 μm	$\sim$28 μm[a]
velocity of macrosteps	$\sim$1600 Å s^{-1}	$\sim$800 Å s^{-1}[a]
Flat layers (facets)		
thickness	1.4 μm	0.9 μm[a]
growth rate v_f	23 Å s^{-1}	29 Å s^{-1}[a]
Growth-rate ratio v_s/v_f	1.7	1.5[a]

[a]After layer No. 6 when steady-state growth was approached.

The transition from misoriented surfaces to facets is energetically favorable. According to Wulff's theorem the equilibrium habit of a crystal consists of faces with the total minimum surface energy.[19] Herring has shown[20] that a hill-and-valley structure lowers the free energy of a misoriented surface, whereas on equilibrium surfaces no hill-and-valley structure should be stable. A crystal growing unconstrained in a solution is finally surrounded by the faces with the lowest growth rates; rough faces with high growth rates disappear. The surface nucleation mechanism is facilitated on the stepped surfaces, under the same supersaturation the facets grow more slowly than the stepped surfaces, and thus become dominant. The development of the equilibrium facet is promoted, as we have lower cooling rates than most LPE growers and thus are nearer to equilibrium.

In conclusion, we have found a gradual transition from stepped misoriented layers to flat facets for misorientations as small as $\frac{1}{6}$° and as large as 0.6°. The absence of macrosteps and other corrugations on the facets influences the effective distribution coefficient and improves the homogeneity of dopant distribution, as indicated by the etching behavior. Growth on facets or on precisely oriented substrates will prevent surface ripples and is likely to increase the performance of LPE-grown semiconductor devices. The required facets can be obtained by *MultiLPE* using low supersaturation, whereas an extremely precise substrate orientation and very low supersaturation would be required in conventional LPE slider techniques due to their inherent geometrical limitation.

The author would like to thank P. Dill for skillful technical assistance, and E. Bauser, E. Courtens, J. R. Jauslin, H. Müller-Krumbhaar, T. Nishinaga, and R. H. Swendsen for fruitful discussions.

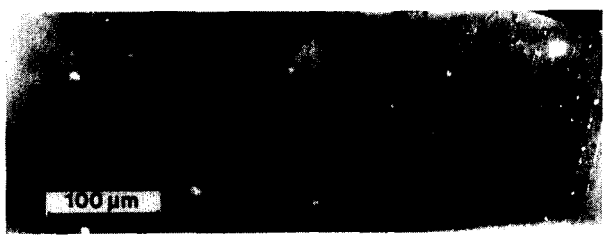

FIG. 3. Composite interference contrast (Nomarski) micrograph of the surface of a facet. The rounded steps of less than 10 Å height and mean distance of 6 μm originate from the edge of the facet.

[1]T. Kajimura, K. Aiki, and J. Umeda, Appl. Phys. Lett. **30**, 526 (1977).

[2]E. Bauser, M. Frik, K. S. Loechner, L. Schmidt, and R. Ulrich, J. Cryst. Growth **27**, 148 (1974).
[3]A. Mottram and A. R. Peaker, J. Cryst. Growth **27**, 193 (1974).
[4]R. C. Peters, *Symposium on Gallium Arsenide 1972*, Inst. Phys. Conf. Ser. **17** (Institute of Physics, London, 1973), p. 55; R. C. Peters and E. André, Acta Electron. **17**, 9 (1974).
[5]K. Pak, T. Nishinaga, and S. Uchiyama, Jpn. J. Appl. Phys. **16**, 949 (1977).
[6]T. Nishinaga, K. Pak, and S. Uchiyama, J. Cryst. Growth **43**, 85 (1978).
[7]D. L. Rode, W. R. Wagner, and N. E. Schumaker, Appl. Phys. Lett. **30**, 75 (1977).
[8]K. Ishida, T. Kamejima, and T. J. Matsui, Appl. Phys. Lett. **31**, 397 (1977).
[9]R. Messham and A. Majerfeld, presented at the 21st Electronic Materials Conference, Boulder, Colorado, 1979, Abstract of Paper G-3 (unpublished).
[10]R. H. Saul and D. D. Roccasecca, J. Appl. Phys. **44**, 1983 (1973).
[11]J. Vilms and J. P. Garrett, Solid State Electron. **15**, 443 (1972).
[12]H. J. Scheel, J. Cryst. Growth **42**, 301, (1970).
[13]T. H. Yeh and A. E. Blakeslee, J. Electrochem. Soc. **110**, 1018 (1963).
[14]P. Dill and H. J. Scheel (unpublished).
[15]B. Fischer, H. J. Queisser, and E. Bauser (private communication, 1977); T. Nishinaga (private communication, 1978).
[16]C. Kimura, T. Yanaki, and H. Hoshino, J. Cryst. Growth **38**, 233 (1977); E. Bauser, L. Schmidt, M. Frik, and K. S. Loechner, *Dreiländer-Jahrestagg. über Kristallwachstum u. Kristallzüchtung*, 1975, KFA Jülich, Report Jul-Conf-18, 1976, KFA Jülich FRG.
[17]H. Tadano, Y. Okuna, M. Shimbo, and J. Nishizawa, J. Cryst. Growth **37**, 184 (1977).
[18]J. R. Jauslin and H. J. Scheel, (unpublished).
[19]D. Elwell and H. J. Scheel, in *Crystal Growth from High-Temperature Solutions* (Academic, New York, 1975), Chap. 5.
[20]C. Herring, Phys. Rev. **82**, 87 (1951).

High-sensitivity InGaAsP/InP phototransistors

M. Tobe and Y. Amemiya
Department of Electronics, Faculty of Engineering, Nagoya University, Furo-cho, Chikusa-ku, Nagoya 464, Japan

S. Sakai and M. Umeno
Department of Engineering Science, Nagoya Institute of Technology, Gokiso-cho, Showa-ku, Nagoya 466, Japan

(Received 13 March 1980; accepted for publication 28 April 1980)

InGaAsP/InP phototransistors have been fabricated using the liquid phase epitaxy technique. In spite of the early stage of development, the fabricated detectors exhibited a current gain of more than 10^3 and rise time of about 50 nsec. With further development, InGaAsP/InP phototransistors will become promising detectors for optical communication systems in the 1.0–1.7-μm spectral region.

PACS numbers: 85.60.Dw, 85.60.Gz, 07.62. + s

Fiber-optic communication in the 1.0–1.7-μm low-loss wavelength region requires detectors with high sensitivity, fast response, and low noise. Ge avalanche photodiodes (APD's) are now the principal detectors in this wavelength region but have large noise because of their high dark current and almost equal ionization coefficients for holes and electrons.[1] InGaAsP/InP APD's have been studied and developed,[2–5] but their relatively large current near breakdown prevents high performance.[6,7] And up to now, an InGaAsP/InP APD with high gain has not been reported except for a special device structure.[8] In this letter, we describe InGaAsP/InP phototransistors with high gain fabricated with the liquid phase epitaxy (LPE) growth technique.

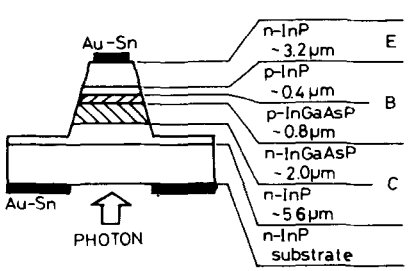

FIG. 1. Schematic cross section of the InGaAsP/InP phototransistor.

Figure 1 shows the structure of the fabricated *n-p-n* phototransistor. Four layers, Sn-doped *n*-InP, Sn-doped *n*-$In_{0.73}Ga_{0.27}As_{0.59}P_{0.41}$ (collector), Zn-doped *p*-InP (base), and Sn-doped *n*-InP (emitter) were grown sequentially on an

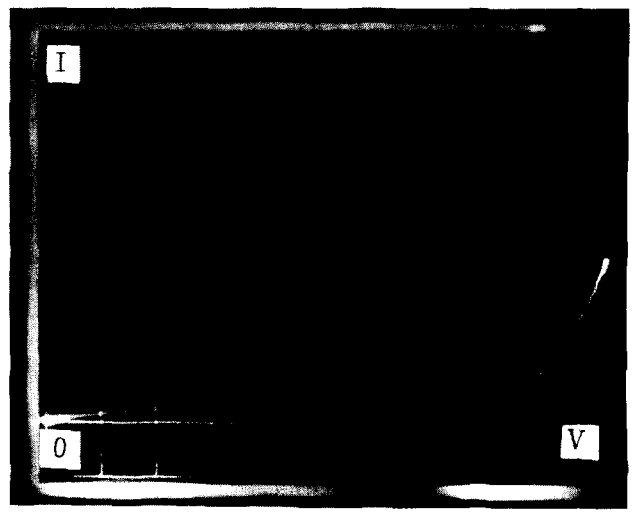

FIG. 2. Current-voltage characteristics of the phototransistor: upper trace, under YAG laser irradiation; lower trace, under dark condition; vertical 2 mA/div, horizontal 0.2 V/div.

 0003-6951/80/130073-03$00.50